Three-dimensional atomic imaging of interface defects between hydrogen-terminated diamond and amorphous Al_2O_3 insulating film

Diamond semiconductor devices are considered ultimate semiconductors. Various methods for creating diamond-based devices, including the use of hydrogen-terminated diamonds (H-diamonds) have been studied. The H-diamond forms a two-dimensional hole gas layer on its surface, which is used as the conduction layer. When manufacturing devices, it is necessary to form an insulating film on their surfaces. Defects at the interface between the insulating film and H-diamond affect the mobility of the device [1], which has gained attention of many researchers. In addition, researchers have shown interest in the atomic arrangement of defects. Fujii *et al.* also studied a method to form an amorphous Al_2O_3 insulating film on the surface using atomic layer deposition with TMA (trimethylaluminum, C_3H_9Al) and DMAH (dimethylaluminum hydride, C_2H_7Al) gases, and found that defects are significantly reduced, especially with DMAH [2]. Therefore, to clarify this difference in the atomic arrangement, we performed photoelectron holography (PEH) at SPring-8 **BL25SU** [2].

Figure 1 shows the C 1*s* X-ray photoemission (XPS) results for the H-diamond with an Al_2O_3 layer grown using TMA and DMAH. The C 1*s* peak comprised three components: C–C, C–H, and C–O. Comparing TMA and DMAH, the C–O peak is reduced in DMAH. It is expected that the C–O bonds correspond to defects. Subsequently, photoelectron holograms were measured. Figure 2 shows the principle of photoelectron holography and a schematic of the retarding field electron energy analyzer (RFA). Photoelectrons are emitted when soft X-rays irradiate a sample. Photoelectrons are scattered by surrounding atoms, and the scattered and unscattered waves interfere, causing interference fringes in the angular distribution of the photoelectrons. These interference fringes are photoelectron holograms that record the three-dimensional atomic arrangement. In addition, it is not necessary for the atomic arrangement to be periodic; thus, it is a powerful tool for measuring dopants [3,4]. The defects with amorphous Al_2O_3 had no periodicity on the diamond surface; however, they could be measured using holography. Furthermore, from the XPS results, the photoelectron hologram of the carbon atom (C–O) bonded to oxygen could be separated by electron energy analysis, making it possible to analyze the atomic arrangement.

Figure 2(b) shows the RFA we developed [5,6]. It comprised three spherical grid electrodes and a screen. A negative retarding voltage was applied to the middle spherical electrode and the first and third spherical grid electrodes were grounded. Photoelectrons with kinetic energies lower than the retarding voltage were reflected by the second electrode. Only the photoelectrons with kinetic energies higher than the retarding voltage passed through the electrode and were projected onto the screen. This RFA is a high-pass filter for electrons and can project photoelectrons of ±50° at once. As it is a high-pass filter, it can be used as a bandpass filter by performing lock-in measurements with various

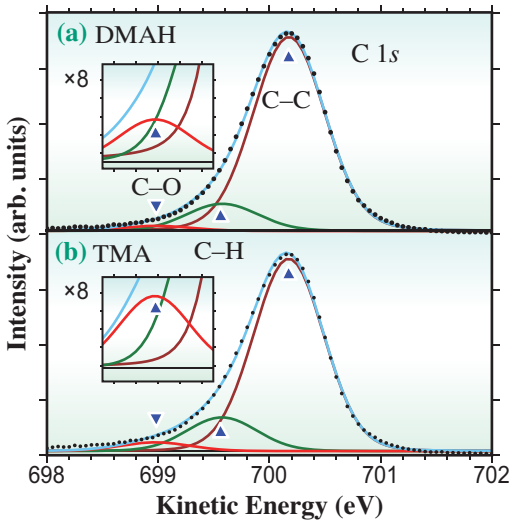

Fig. 1. C 1*s* XPS of Al_2O_3 / H-diamond. **(a)** DMAH. **(b)** TMA.

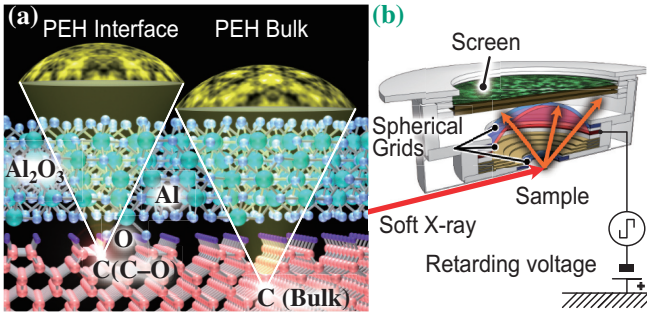

Fig. 2. **(a)** Recording process of photoelectron holography. **(b)** Retarding field analyzer for photoelectron holography.

retarding voltages. We modified the arrangement of the spherical grids to obtain a high resolution of E/ΔE~2000. This is approximately 10 times the resolution of the commercial products.

We observed the photoelectron hologram for all XPS measurement points in Fig. 1 and measured the kinetic energy dependence of the photoelectron hologram. By peak fitting these data, we obtained holograms of each component of C–C, C–H, and C–O.

This is shown in Fig. 3(a), where C–C represents the photoelectrons emitted by the bulk carbon atoms of the diamond. A simulation was performed on the photoelectron hologram of bulk diamond. The simulation used the total-analysis multiple scattering pattern (TMSP) program package in the 3D-AIR-IMAGE software developed by the author, as shown in Fig. 3(a) Sim., which was found to be ideal. Figure 3(c) shows the hologram of C–O. In addition, a newly developed atomic image reconstruction algorithm was used to regenerate the three-dimensional atomic image, as shown in Figs. 4(b,c). By analyzing this atomic image, the atomic arrangement shown in Fig. 4(a) was estimated. A hydrogen-terminated diamond surface formed two rows of hydrogen dimers. A C–O–Al–O–C bond was formed to bridge the two dimer rows. This atomic arrangement information is important for the future development of diamond devices.

In addition, photoelectron holography can measure not only the atomic arrangement of dopants but also the reduction arrangement of the crystal-amorphous interface. Photoelectron holography will exert great power in future surface and interface analyses.

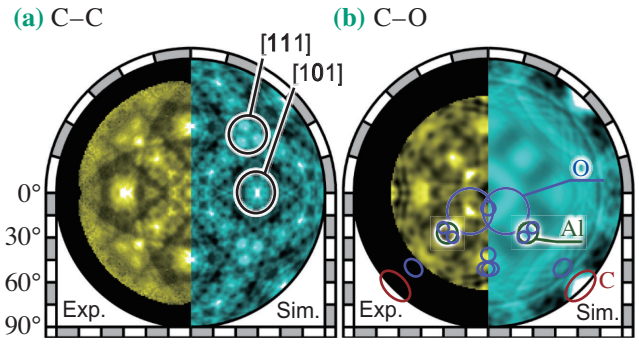

Fig. 3. **(a)** PEH of C–C. Exp. and Sim. are the experimental result and simulated result, respectively. **(b)** PEH of C–O, that is, defect at the interface between H-diamond and Al_2O_3 amorphous layer.

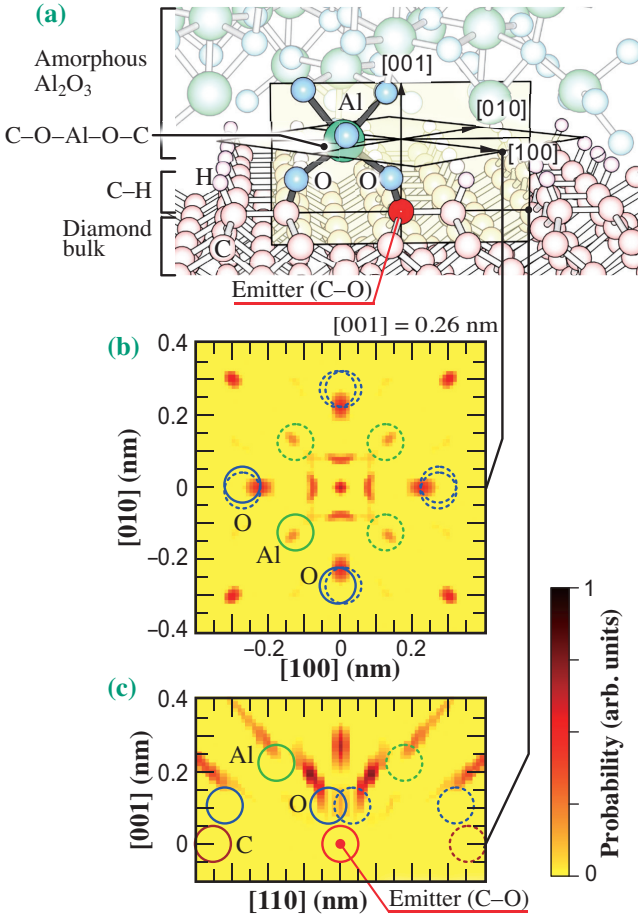

Fig. 4. Atomic arrangement of the defect between H-terminated diamond and Al_2O_3 amorphous layer.

T. Matsushita[a,*], Y. Hashimoto[a], M. N. Fujii[b] and J. Mizuno[c,d]

[a] Graduate School of Science and Technology, Nara Institute of Science and Technology
[b] Faculty of Science and Engineering, Kindai University
[c] Research Organization for Nano and Life Innovation, Waseda University
[d] Academy of Innovative Semiconductor and Sustainable Manufacturing, National Cheng Kung University, Taiwan

*Email: t-matusita@ms.naist.jp

References

[1] W. Fei *et al.*: Appl. Phys. Lett. **116** (2020) 212103.
[2] *M. N. Fujii, M. Tanaka, T. Tsuno, Y. Hashimoto, H. Tomita, S. Takeuchi, S. Koga, Z. Sun, J. I. Enriquez, Y. Morikawa, J. Mizuno, M. Uenuma, Y. Uraoka and T. Matsushita: Nano Lett.* ***23*** *(2023) 1189.*
[3] T. Yokoya *et al.*: Nano Lett. **19** (2019) 5915.
[4] K. Tsutsui *et al.*: Nano Lett. **17** (2017) 7533.
[5] T. Muro *et al.*: J. Synchrotron Rad. **28** (2021) 1669; T. Muro *et al.*: Rev. Sci. Instrum. **88** (2017) 123106.
[6] T. Matsushita *et al.*: J. Phys. Soc. Jpn. **87** (2018) 061002.